ELSEVIER

Biochimica et Biophysica Acta 1236 (1995) 228–236

BBA Biochimica et Biophysica Acta

Dispersion state of phospholipids and fluorescence production with peroxidation in organic solvents: investigated by time-resolved fluorescence technique

Jin-Ye Wang [a,*], Ken-ichiro Suzuki [b], Tetsuro Fujisawa [a], Tatzuo Ueki [a], Tsutomu Kouyama [a]

[a] *Biophysics Laboratory, The Institute of Physical and Chemical Research, Wako, Saitama 351-01, Japan*
[b] *Japan Collection of Microorganisms, The Institute of Physical and Chemical Research, Wako, Saitama 351-01, Japan*

Received 12 December 1994; revised 6 February 1995; accepted 6 February 1995

Abstract

Fluorescent substances were found to be produced efficiently when phospholipids containing phosphatidylethanolamine (PE) and linoleic chains were autoxidized in non-polar solvents. By using these fluorescent substances as intrinsic probes, the dispersion state of phospholipids was investigated in various organic solvents. Fluorescence anisotropy decay measurements indicated that the aggregation size of phospholipids was much larger in hexane than in chloroform, methanol and *tert*-butyl alcohol. The average diameter of phospholipid aggregates in hexane was calculated to be 4–6 nm, which was dependent on the lipid composition. A consistent result was obtained when *N*-(7-nitrobenz-2-oxa-1,3-diazol-4-yl)-1,2-dihexadecanoyl-*sn*-glycero-3-phosphoethanolamine (NBD-PE) was used as an extrinsic probe. Comparison of the fluorescence data with small-angle X-ray scattering (SAXS) data suggested that a reverse micellar structure of phospholipids formed in hexane. It was shown that phospholipid aggregation enhanced the extent of peroxidation as well as the production yield of fluorescent substances of phospholipids.

Keywords: Amino phospholipid; Fluorescence anisotropy; Peroxidation; Aggregation; Reverse micelle

1. Introduction

Reaction of lipid oxidation products with primary amino compounds produces fluorescent substances. This reaction has been shown to be responsible for accumulation of fluorescent pigments in aged cells [1–4]. Although the fluorescence method has been widely used to assay lipid peroxidation, formation mechanisms of fluorophores are poorly understood. Most studies have been carried out with model systems containing water-soluble amino compounds and oxidation products of linoleic acid. On the other hand, amino phospholipids are the major components of biomembranes, and their participation in pigment production has been observed in artificial [5] and biological membrane systems [6–9]. These studies have suggested that lipid oxidation products reacting with amino groups are short-lived and inactivated in the aqueous phase. It is anticipated that the production efficiency of fluorophores is influenced by many factors including the dispersion state of phospholipids. Phospholipids in water organize in the form of a bilayer, and they form reverse micellar structures in a variety of organic solvents. A reverse micellar structure may also occur transiently within the bilayer structure of a biological membrane that is undergoing large-scale morphological changes such as fusion [10]. We consider that the reverse micelles formed by phospholipid mixtures in organic solvents are a useful model for studies of the formation mechanism of fluorophores during lipid peroxidation.

In the present study, synthesized phospholipids with known fatty acid compositions were autoxidized in various organic solvents, and the fluorescent substances produced by peroxidation were utilized as the intrinsic probe for

Abbreviations: AOT, aerosol bis(2-ethylhexyl)sulfosuccinate sodium salt; DLPC, L-α-phosphatidylcholine dilinoleoyl; DLPE, L-α-phosphatidylethanolamine dilinoleoyl; DOPE, L-α-phosphatidylethanolamine dioleoyl; NBD-PE, *N*-(7-nitrobenz-2-oxa-1,3-diazol-4-yl)-PE; PLPE, L-α-phosphatidylethanolamine 1-palmitoyl-2-linoleoyl; PLPC, L-α-phosphatidylcholine 1-palmitoyl-2-linoleoyl; SAXS, small-angle X-ray scattering; TLC, thin-layer chromatography.

* Corresponding author. Present address: Photobiology Group, Photodynamics Research Center, The Institute of Physical and Chemical Research (RIKEN), Sendai, Japan. Fax: +81 22 2282045.

SSDI 0005-2736(95)00052-6

investigation of the dynamic structure of peroxidized phospholipids in solvents with different polarities. An extrinsic probe, *N*-(7-nitrobenz-2-oxa-1,3-diazol-4-yl)-1,2-dihexadecanoyl-*sn*-glycero-3-phosphoethanolamine (NBD-PE) was also used to study the dispersion state of phospholipids before and after oxidation. Another piece of information of lipid aggregation was obtained by small-angle X-ray scattering (SAXS) measurements. On the basis of the results obtained, a possible effect of the dispersion state of phospholipids on their autoxidation is discussed.

2. Materials and methods

2.1. Materials

L-α-Phosphatidylcholine dilinoleoyl (DLPC), L-α-phosphatidylcholine 1-palmitoyl-2-linoleoyl (PLPC), L-α-phosphatidylethanolamine dilinoleoyl (DLPE), L-α-phosphatidylethanolamine 1-palmitoyl-2-linoleoyl (PLPE), L-α-phosphatidylethanolamine dioleoyl (DOPE) were purchased from Avanti Polar Lipids (Alabaster, AL). All phospholipids gave single spots on silica gel thin-layer chromatography (TLC). NBD-PE was from Molecular Probes (Eugene, OR).

2.2. Peroxidation procedure

0.5 mM of phospholipid in organic solvent in a test tube was incubated at 37° C in the dark. After various periods of autoxidation, the amounts of conjugated diene and oxodiene were determined from absorbances at 234 nm and 270 nm, respectively, with a Shimadzu UV2000 spectrophotometer [11]. Fatty acid composition of phospholipids before and after oxidation was analyzed by the capillary gas-liquid chromatography after methylation, using heptadecanoic acid as an internal standard [12].

2.3. Separation of fluorescent substances

Fluorescent substances produced by autoxidation were separated by the reversed phase TLC (RP18, Merck) using chloroform/methanol/water (1:10:0.5, v/v) as a developing solvent. Fluorescent bands were scraped and fluorescent substances were extracted by chloroform/methanol (2:1, v/v). They were separated further by the normal phase TLC (K6, Whatman) using chloroform/methanol/water (65:25:4, v/v) as a developing solvent. Spots on a TLC plate were detected with Dittmer reagent (for phospholipids), ninhydrin spray (for primary and secondary amino groups) and a UV lamp (for fluorescent spots). Corrected fluorescence spectra were measured with a Hitachi 650-60 fluorometer. The fluorescence quantum yield of the oxidation products was calculated by using 0.1 μM quinine sulfate in 0.1 M sulfuric acid as a standard fluorophore. Its quantum yield was assumed to be 0.55. Fluorescence intensity profile on a TLC plate was measured with a special attachment of the spectrofluorometer.

2.4. Time-resolved fluorescence anisotropy measurements

Fluorescence intensity and anisotropy decays were measured with a single-photon counting fluorometer [13]. Nanosecond light pulses provided by free-running discharge in hydrogen gas at 11 MPa were polarized vertically with a Glan prism. Two beams of fluorescence emitted at 90° to the excitation beam was collected, and vertically and horizontally polarized components of fluorescence, $I_{\parallel}(t)$ and $I_{\perp}(t)$, were measured simultaneously with 2 photomultiplier tubes. Experimental decay curves of fluorescence anisotropy were computed as follows:

$$r_{ex}(t) = \left(I_{\parallel}(t) - I_{\perp}(t)\right)/\left(I_{\parallel}(t) + 2I_{\perp}(t)\right) \equiv D(t)/S(t) \quad (1)$$

A sample containing autoxidation products was excited at 360 nm and emission above 460 nm was collected. A sample containing NBD-PE was excited at 460 nm and emission above 540 nm was collected.

2.5. Analysis of fluorescence data

A multiexponential function $s(t)$ was employed to fit an experimental decay curve of the total intensity $S(t)$.

$$s(t) = \sum_{i=1}^{N} a_i \exp(-t/\tau_i) \quad (2)$$

where $s(t)$ is the total fluorescence intensity at time t after an infinitely short light pulse, τ_i is the lifetime for the i-th component, a_i is the decay amplitude for τ_i, and N is the total number of the components. The maximum value of i is 3 in the present calculations.

The decay of anisotropy $r(t)$ was assumed to be a single (or double) exponential function.

$$r(t) = r_0 \exp(-t/\theta) \quad (3)$$

where r_0 is the fundamental anisotropy that would be observed in the absence of motion, and θ is the rotational correlation time under mono-exponential approximation. In the rigid rotator model, the correlation time, θ is proportional to the volume of the rotator:

$$\theta = kTv/\eta \quad (4)$$

where k is the Boltzmann constant, T the absolute temperature, and η the viscosity of the surrounding medium. Since T and η are experimental quantities, one can estimate the size of the rotator v from the correlation time [14].

2.6. Small-angle X-ray scattering measurements

X-ray from a conventional laboratory generator was used for the SAXS experiment. Detailed optics were de-

scribed elsewhere [15]. Cu Kα radiation ($\lambda = 0.154$ nm) was used and diffraction spacing was calibrated with cholesterol. The sample to specimen distance was about 460 mm. The sample cell was washed thoroughly with solvent before measurements. The temperature was maintained at 34° C in order to keep *tert*-butyl alcohol in the liquid state. The scattering intensity $I(S)$, where S equals to $2\sin\theta/\lambda$, 2θ is a scattering angle and λ is a wavelength, was analyzed using S^2 vs. $\ln(I(S))$ plot (the Guinier plot) [16]. The linear region in inner scattering angle gives the radius of gyration defined by:

$$R_g^2 = \int |\vec{r}|^2 \rho(\vec{r}) dV_r / \int \rho(\vec{r}) dV_r \quad (5)$$

where $\rho(\vec{r})$ is the excess electron density of a molecule. The maximum dimension of the particle, D_{max}, was calculated from inverse Fourier transformation of scattering intensity profile:

$$P(r) = 8\pi r \int_0^\infty SI(S)\sin(2\pi Sr) dS \quad (6)$$

$P(r)$ is the distance distribution function; i.e., the distribution of electron pair distance inside the molecule. The first zero-crossing point of $P(r)$ is the maximum dimension of the particle.

3. Results

3.1. Oxidation of phospholipids in organic solvents

Phospholipids were incubated at 37° C in hexane, chloroform, *tert*-butyl alcohol and methanol and oxidation products were assayed after various incubation periods. Table 1 shows the amounts of conjugated diene, oxodiene and fluorescent substances generated by autoxidation for 10–12 days. Large amounts of conjugated diene and oxodiene were generated when PLPC, DOPE/PLPC, DLPC, and DOPE/DLPC were dispersed in hexane. The consumption rate of the linoleic chain was high (18–41%) in hexane, slightly lower (16%) in chloroform, and very low (0–2%) in alcohols.

Phospholipid without amino group (PLPC and DLPC) scarcely generated fluorescent compounds. Oxidation of DOPE yielded a negligible amount of fluorescent substances. When the mixture of DOPE and DLPC (or PLPC) was oxidized in hexane, however, fluorescent substances were produced efficiently. A high production efficiency of fluorescent substances was also observed when phospholipid containing both amino group and linoleic chain (PLPE and DLPE) were oxidized in chloroform. Production of fluorescent substances was negligible in alcohols. It should be noticed that, in chloroform, the amount of fluorophores produced from DOPE/PLPC (or DOPE/DLPC) was considerably lower than that observed for PLPE (or DLPE). This difference will be discussed later in relation with the dispersion state of phospholipids.

Table 1
Diene, oxodiene and fluorescent substances produced by phospholipid autoxidation in different reaction phases

	Oxidation (day)	$(C=C)_2$ [a]	$C(=O)\text{-}(C=C)_2$ [b]	ΔFI [c]
Hexane				
DOPE	10	–	–	0.002
DLPC	10	0.082	0.027	0.096
DOPE/DLPC	10	0.137	0.087	8.208
DLPE [d]	10	0.038 [d]	0.027 [d]	0.950 [d]
PLPC	12	0.106	0.038	0.005
DOPE/PLPC	12	0.080	0.040	0.209
PLPE [d]	10	0.016 [d]	0.008 [d]	0.048 [d]
Chloroform				
DOPE	10	–	–	0.012
DLPC	10	0.026	0.010	0.000
DOPE/DLPC	10	0.063	0.018	1.083
DLPE	10	0.054	0.033	3.833
PLPC	12	0.038	0.026	0.004
DOPE/PLPC	12	0.054	0.034	0.160
PLPE	10	0.086	0.030	0.958
t-BuOH				
PLPC	12	0.030	0.026	0.000
DOPE/PLPC	12	0.032	0.028	0.012
Methanol				
DOPE	10	–	–	0.002
DLPC	10	0.011	0.006	0.000
DOPE/DLPC	10	0.014	0.011	0.023
DLPE	10	0.018	0.008	0.038
PLPC	12	0.011	0.006	0.000
DOPE/PLPC	12	0.014	0.011	0.023
PLPE	10	0.013	0.009	0.064

The concentration of each phospholipid was 0.5 mM. Oxidation was carried out at 37° C in the dark for 10 or 12 days, and the oxidation products were assayed in methanol.

[a] μmol of $(C=C)_2$ per μmol linoleic chain, $\lambda = 234$ nm ($\epsilon = 28000$ M^{-1} cm^{-1}).

[b] μmol of $C(=O)\text{-}(C=C)_2$ per μmol linoleic chain, $\lambda = 270$ nm ($\epsilon = 20000$ M^{-1} cm^{-1}).

[c] Fluorescence intensities were measured with excitation at 360 nm and emission at 430 nm and were corrected for with 0.1 μM quinine sulfate in 0.1 M sulfuric acid. The data present changes in fluorescence intensity induced by incubation for 10 or 12 days.

[d] DLPE and PLPE in hexane was found to be deposited partly on a wall of the test tube with oxidation, and the values indicate the amount of oxidation products dissolving in the solvent.

t-BuOH, *tert*-butyl alcohol.

3.2. Analyses of the fluorescent substances by TLC

The reversed phase TLC of the autoxidized DOPE/PLPC mixture gave one major band which emitted pale blue light upon illumination with the UV lamp at 366 nm (Fig. 2d). This band was located at slightly lower position than unoxidized PE (Fig. 1a); most non-fluorescent oxidation products (i.e., phospholipid hydroperoxides) appeared at much higher positions. When the fluorescence band was scraped and applied to the normal phase TLC, it was separated into two major bands (Band I and II) and one minor band (Band III); the intensity profile of fluorescence is shown in Fig. 1b. Band I, which appeared near the top, exhibited an emission spectrum with a fine structure in hexane (Fig. 2a). With increase of the

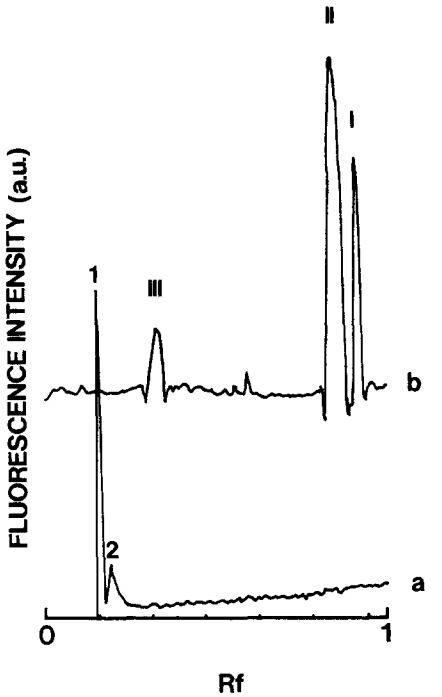

Fig. 1. Thin-layer chromatograms of oxidized DOPE/PLPC. Phospholipids were autoxidized in chloroform for 12 days at 37° C. The first separation (a) was carried out by a reversed phase TLC (RP18) with a developing reagent chloroform/methanol/water (1:10:0.5, v/v). The second separation (b) of band 1 was carried out by a normal phase TLC (K6) with a developing reagent chloroform/methanol/water (65:25:4, v/v). Fluorescence intensity was measured with excitation at 360 nm and emission at 430 nm.

polarity of solvent, the fine structure smeared out and the center of the emission spectrum was slightly red-shifted. Band I and II exhibited broad emission spectra in a similar wavelength region as that of Band I (Fig. 2b,c). A small red-shift of the emission maximum was observed when the polarity of solvent was increased. The fluorophore in Band II was unstable in air, and it was partly decomposed into a compound which was indistinguishable spectroscopically from the fluorophore in Band I. It is possible that the fluorophore in Band I is generated from the one in Band II. It should be noted that corrected excitation spectra of all these fluorescent compounds have maximal intensities near 360 nm. The absorption increase at this wavelength was much smaller than the absorption increases at 234 nm or 270 nm which are due to formation of diene or oxodiene. Nonetheless, the fluorescence intensity observed was not very weak as compared to that of 0.1 μM quinine sulfate. The fluorescence quantum yield of the fluorophore in Band II was estimated to be approx. 0.2 in methanol.

The lower fluorescence intensity in hexane than in methanol for separated Band I, II and III may be due to a partial self-quenching of fluorophores which are capable of aggregation in hexane (see below). This is more obvious for NBD-PE which is non-fluorescent in hexane. However, coexistence of other phospholipids resulted in a contrary effect, i.e., the fluorescence intensity in hexane is higher than in methanol for both mixtures of Band I, II, III (Fig. 2d) and NBD-PE (data not shown). The result indicated that these fluorescent products and NBD-PE are highly fluorescent when diluted by other phospholipids in aggregation state.

Although fluorophores were also produced in phospholipid dispersions containing no amino group, their production has to be explained by a different reaction pathway [17,18]. The fluorescence emission spectra of oxidized DLPC exhibited an maximal intensity around 460 nm and were largely red-shifted as compared with the emission spectra of oxidized DLPE or DOPE/PLPC.

3.3. Time-resolved fluorescence measurements of oxidized phospholipids

For time-resolved fluorescence measurements, phospholipids oxidized for 4–12 days in chloroform were re-dissolved in various organic solvents. Fig. 3 shows a typical example of fluorescence intensity and anisotropy decay curves of oxidized samples. The fluorescence intensity decay curves were described well by two exponential

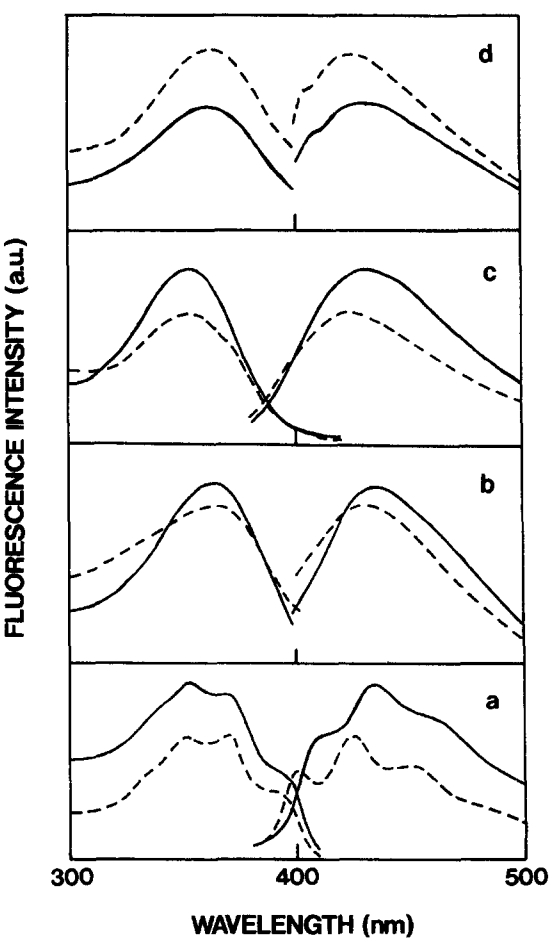

Fig. 2. Corrected fluorescence spectra of peroxidized DOPE/PLPC before separation (d), Band I (a), Band II (b), Band III (c) in different organic reagents. (- - -) hexane; (—) methanol.

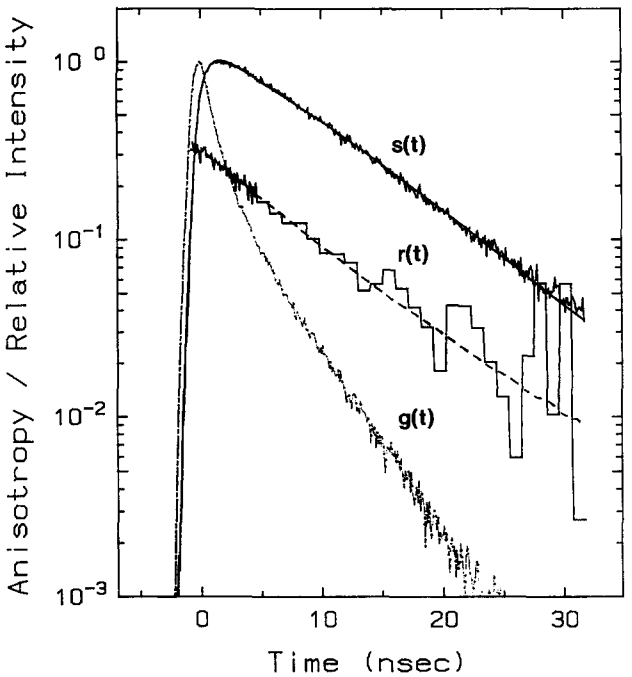

Fig. 3. Fluorescence intensity and anisotropy decay curves of peroxidized DOPE/PLPC in hexane. The total intensity decay $s(t)$ (dots) was fitted with a double-exponential function (solid line): $\tau_1 = 1.36$ ns, $a_1 = 0.47$, $\tau_2 = 7.93$ ns, $a_2 = 0.53$. The anisotropy decay (zigzag curve) was fitted with a single-exponential function (broken line): $\theta = 5.06$ ns, $r_0 = 0.337$. The chain line represents the response function of the apparatus.

components. The fast decaying component has a lifetime of 1–2 ns and the slow component has a lifetime of 6 to 9 ns, which decreased with increase of the polarity of solvent (Table 2). For samples before separation by TLC, the two decay components have approximately equal amplitudes. But the fast component was dominant in the fluorescence intensity decay curve of Band I. This indicates that the multiple lifetimes come from heterogeneity of the fluorophores generated by autoxidation. The intensity decay curves of Band II were characterized by a relatively larger amplitude of the slow component, but the result varied from preparation to preparation probably because the fluorophore in Band II was unstable.

In most cases, fluorescence anisotropy decay curves of oxidized samples were described well with a single exponential component, irrespective of the multiplicity of lifetime. This suggests that most of the fluorophores existing in oxidized phospholipids have similar dynamic properties. An exceptional case was observed when oxidized DLPE was dispersed in hexane. In this case, deviation from a single exponential decay was significant. Except for such a special case, the rotational correlation time observed is interpreted straightforwardly; i.e., it is expected to reflect the dynamic structures of fluorophores or objects anchoring them. If it is assumed that phospholipids aggregate to form a spherical assembly in which a fluorophore is fixed rigidly, the aggregate size can be evaluated by using Eq. (4). On this assumption, the diameter of aggregation can be calculated to be 5.1–5.6 nm in hexane, 2.6–2.8 nm in chloroform and 1.8–2.3 nm in alcohols (the last column in Table 2). The aggregate size of DLPE in hexane appeared to be smaller (4.4 nm) than those observed for the other lipids. Even when such a variation in the evaluated size is

Table 2
Fluorescence data of peroxidized PE in organic solvents

Sample	Solvent	Temperature (° C)	η (cP)	a_1	τ_1 (ns)	a_2	τ_2 (ns)	$\langle\tau\rangle$ (ns)	r_0	θ (ns)	R (nm)
DOPE/PLPC	hexane	34	0.305	0.48	1.66	0.52	8.16	7.25	0.332	5.1 (1.1)	2.57(0.19)
	chloroform	34	0.583	0.45	1.76	0.55	7.34	6.59	0.288	1.2 (0.1)	1.28(0.03)
	t-BuOH	34	2.781	0.47	2.10	0.53	7.71	6.74	0.296	4.1 (0.3)	1.14 (0.03)
	methanol	34	0.504	0.66	2.09	0.34	6.52	5.05	0.326	0.4 (0.1)	0.93 (0.08)
DLPE	hexane	34		0.51	2.09	0.49	8.04	7.14	0.354	3.1 (0.6)	2.17 (0.14)
	chloroform	34		0.43	2.24	0.57	7.30	6.43	0.300	1.5 (0.1)	1.38 (0.03)
	t-BuOH	34		0.47	1.76	0.54	7.58	6.74	0.296	5.8 (0.7)	1.28 (0.05)
	methanol	34		0.69	2.49	0.31	6.73	4.99	0.265	0.7 (0.1)	1.12 (0.05)
Band I	chloroform	34		0.95	1.38	0.05	8.90	3.42	0.171	0.5	0.95
	methanol	34		0.96	1.30	0.04	9.41	3.34	0.182	0.3	0.84
DOPE/DLPC	hexane	22	0.324	0.65	3.17	0.45	8.98	7.24	0.325	7.6	2.84
	chloroform	22	0.624	0.54	1.27	0.46	7.32	6.37	0.292	1.8	1.41
	methanol	22	0.578	0.60	1.56	0.40	6.35	5.26	0.284	0.8	1.10
DLPE	hexane	22		0.60	1.74	0.40	8.49	7.15	0.297	3.7	2.23
	chloroform	22		0.54	2.60	0.46	7.97	6.47	0.258	1.8	1.41
	methanol	22		0.66	1.53	0.34	7.05	5.58	0.289	0.5	1.10
PLPE	hexane	22		0.67	0.89	0.33	7.57	6.56	0.306	6.8	2.74
	chloroform	22		0.50	1.36	0.50	7.22	6.38	0.292	1.9	1.44
	methanol	22		0.67	3.20	0.33	7.72	5.71	0.259	0.6	1.01

Phospholipids were oxidized at 37° C in chloroform for 4–12 days, then re-dissolved in various organic solvents. Band I was separated from autoxidized DOPE/PLPC by TLC.

τ_1, τ_2 and a_1, a_2 are fluorescence lifetimes and relative amplitudes obtained by double-exponential fitting. $\langle\tau\rangle$ is obtained by the moment method. r_0 is the fundamental anisotropy. Fluorescence anisotropy decays are analyzed with a single time constant θ for most samples, except that double-exponential approximation is used for DLPE systems, and the θ is expressed as $(b_1/\theta_1 + b_2/\theta_2)^{-1}$. R is the radius of phospholipid particles calculated by Eq. (4). Standard deviation is in parentheses.

taken into consideration, the aggregate size in hexane is much larger than the length of each phospholipid molecule with straight hydrocarbon chains. It is thus suggested that the number of phospholipids incorporated into each aggregate is large. (The aggregation number may be 50–100 if phospholipids are closely and rigidly packed.) In the other solvents investigated, on the other hand, this number should be much smaller. It seems likely that only the monomeric form of phospholipid exists in alcohols.

Formation of large aggregates of phospholipids in hexane was confirmed by using an extrinsic fluorescent probe, NBD-PE. When a small amount of NBD-PE was added to a phospholipid dispersion (1:100 molar ratio), the fluorescence anisotropy decay curve was described with a single exponential component. A slight decrease in the rotational correlation time was found when the labeled DOPE/PLPC was incubated at 37° C for 8 days, but this change may be within experimental error. On the same assumption as used above, it is calculated from the rotational correlation times of the labeled samples that the diameter of phospholipid aggregates in hexane is 5.0 nm for DOPE/PLPC and 4.4 nm for DLPE (Table 3). These values are close to the values evaluated from the anisotropy decays of the intrinsic fluorophores. It is thus concluded that phospholipids form large aggregates in hexane. In alcohols, on the other hand, a noticeable difference in the rotational correlation time was found for the intrinsic and extrinsic fluorophores. A much shorter correlation time (< 0.1 ns) was observed for NBD-PE and this may be explained by assuming that intramolecular motion of NBD-PE becomes significant when it exists in a monomeric state. A slight difference in the rotational correlation time was also found when fluorophores in Band I, II and III were examined in methanol. The fluorophore in Band I was suggested to have a shorter hydrocarbon chains than those in Band II and III.

3.4. Small-angle X-ray scattering measurements

In Fig. 4, SAXS data of fresh dispersions of DOPE/PLPC and DLPE in hexane are displayed. A good linearity to inner scattering angle is seen in the Guinier plots, indicating monodispersity of lipid aggregation. The R_g value of aggregates of DOPE/PLPC was determined to be 1.74 nm (± 0.08) nm. A slightly smaller value (1.43 ± 0.17 nm) was obtained for DLPE. Since the electron density of the lipid hydrocarbon chains is close to that of the solvent, the lipid polar group contributes to the X-ray scattering more significantly than the hydrocarbon chain moiety does. This should be taken into consideration when the SAXS result is compared with the fluorescence result. By using Eq. (6), the D_{max} values of DOPE/PLPC and DLPE aggregates were evaluated to be 5.0 (± 0.2) nm and 4.0 (± 0.2) nm, respectively. There is no significant difference between the D_{max} value and the aggregation size evaluated from the fluorescence anisotropy data. It

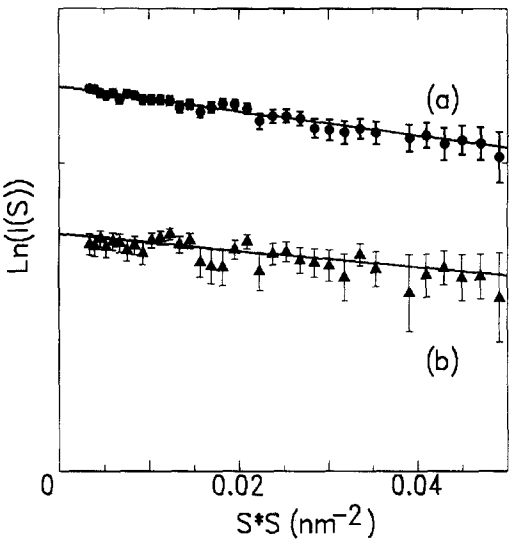

Fig. 4. Guinier plot for phospholipids dispersed in hexane. The concentrations of DOPE/PLPC (a) and DLPE (b) are the same as those used in the fluorescence experiment. Error bars show one sigma of each point. The R_g values of DOPE/PLPC and DLPE are determined to be 1.74 nm (0.08 nm) and 1.43 nm (0.17 nm), respectively.

Table 3
Fluorescence data of NBD-PE/phospholipid in organic solvents (34° C)

Sample	Solvent	Oxidation (day)	τ (ns)	r_0	θ (ns)	R (nm)
DOPE/PLPC	hexane	0	10.28	0.306	4.7 (0.4)	2.50 (0.07)
	hexane	8	11.40	0.310	4.0 (0.2)	2.37 (0.04)
	chloroform	0	8.53	0.161	1.1 (0.1)	1.24 (0.04)
	t-BuOH	0	7.55	0.300	0.7	0.63
	methanol	0	5.29	0.389	< 0.1	< 0.58
DLPE	hexane	0	11.50	0.311	3.1 (0.1)	2.17 (0.02)
	chloroform	0	9.53	0.228	1.4 (0.2)	1.34 (0.06)
	t-BuOH	0	8.74	0.244	1.2	0.76
	methanol	0	5.29	0.345	0.1	0.58

The ratio of NBD-PE to phospholipids was 1:100.
Both the fluorescence lifetime τ and correlation time θ are obtained under single exponential approximation. r_0 is the fundamental anisotropy. R is the radius of phospholipid particles calculated by Eq. (4). Standard deviation is in parentheses.

should be noticed that the observed R_g values are much smaller than the values that would be expected if the electron density was assumed to be uniform within the aggregation; e.g., $R_g = 1.94$ nm for a uniform sphere with a diameter of 5.0 nm. Thus, the experimental data suggested that the lipid polar groups occupy the inner part of the aggregate.

The phospholipid mixture in *tert*-butyl alcohol gave a poor SAXS signal. The R_g value was small (0.8 nm). This suggests that no large aggregate of phospholipids is formed in this solvent.

4. Discussion

4.1. Dispersion state of phospholipids in various organic solvents

Reverse micelles of surfactants in an organic phase have been studied in detail by various methods including fluorescence technique. For example, reverse micelles of a classic ionic surfactant, aerosol bis(2-ethylhexyl)sulfosuccinate sodium salt (AOT) in n-heptane and n-dodecane at various values of $W = [H_2O]/[AOT]$ have been investigated by monitoring the decay of the total fluorescence and the fluorescence anisotropy of cresyl violet [19]. Until now, however, little has been done on the study of the form and size of the phospholipid aggregates until now [20]. Our present result indicates that fluorescent substances produced by lipid peroxidation can be used as intrinsic probes for determination of the dispersion state of oxidized phospholipids. It is shown from time-resolved fluorescence polarization measurements that phospholipids form a much larger aggregate in hexane than in chloroform and alcohols. The SAXS data confirm the result and suggest a reverse micellar structure of phospholipid mixtures in hexane. The average diameter of reverse micelles was evaluated to be 5.0 nm for DOPE/PLPC. A smaller aggregation size (4.4 nm) was suggested for a fresh sample of DLPE. It is possible that the micellar size is influenced by the lipid composition as well as the shape of each lipid component. On the other hand, the fluorescence anisotropy decay of oxidized DLPE in hexane was not described well with a single exponential function. Deviation from a single exponential decay can be explained if fluorophores undergo a restricted internal motion within micelles. A more likely explanation is, however, that the size distribution of the micelles becomes broader as the lipid peroxidation proceeds. In this relation, we observed that very large insoluble aggregates of oxidized lipids appeared on the wall of the test tube when DLPE in hexane was oxidized for a long period. The micelles of DLPE seem to get an agglutinative property upon oxidation.

It has been reported that phospholipids in chloroform exist as monomers at the lipid concentration used in the present study (0.5 mM), though they form small aggregations at a much higher lipid concentration [21]. No evidence for phospholipid aggregation in methanol and *tert*-butyl alcohol has been obtained [22]. It is thus more realistic to consider that the fluorescence anisotropy decays of oxidized phospholipids observed in these solvents represent the rotational motion of the fluorophores themselves rather than that of phospholipid aggregates. If it is assumed that the fluorophores do not associate with other phospholipids, it would be suggested from the rotational correlation time that they have an molecular size of 2.0–2.6 nm (Table 2). This molecular size may be expected for a lipid-chromophore with long hydrocarbon chains. Although a slightly larger molecular size was evaluated in chloroform than in the alcohols, such a small difference can be explained if the fluorophores take different conformations in different solvents. Strictly speaking, the rotational correlation time is dependent on the shape of a fluorophore as well as the orientation of transition dipole moments with respect to the principal axes of the molecule [23] and it may be meaningless to use the fluorescence anisotropy data for further characterization of the fluorophores. Nonetheless, it is important to note that intramolecular motion of the intrinsic fluorophores is very restricted. In the case of NBD-PE, a flexible configuration was suggested from the short rotational correlation time observed in methanol (< 0.1 ns).

4.2. Effect of the dispersion state of phospholipids on their autoxidation

Topological control of reactivity has been an extensive subject for chemists. Some reactions such as photodimerization have shown to be limited in solution by a lack of stereochemical or regiochemical selectivity, and high yields of photodimers in micellar media [24]. Oxidation of PC in non-polar organic solvents has been reported to be enhanced by the formation of reverse phase micelles. This was explained by close packing of lipids which facilitates propagation of the radical chain reaction [22]. Moreover, the fact that the oxidizability of reverse DLPC micelles when mixed with saturated DPPC micelles is lower than that of DLPC reverse micelles alone can be attributed to the dilution of DLPC by DPPC due to fast and efficient exchange of phospholipids between micelles [25]. The present study shows that the oxidation of phospholipids with polyunsaturated hydrocarbon chains is higher in hexane than in the other solvents (Table 1). A higher oxidation extent in hexane is attributable to formation of reverse micelles, though the very low oxidation rate in alcohols may be due to their scavenging function to hydroxy radicals [26].

Co-existence of amino groups and polyunsaturated hydrocarbon chains in solution is shown to be a requisite for production of fluorescent substances. This indicates that most fluorophores are produced by reaction of the amino group of PE with secondary oxidation products of the

polyunsaturated chains. It is therefore interesting to investigate how the dispersion state of phospholipids affects the production efficiency of fluorophores, especially in the lipid mixture system DOPE/DLPC or DOPE/PLPC. The result shown in Table 1 indicates that, in chloroform, the production efficiency of fluorophores is much smaller in DOPE/DLPC (or DOPE/PLPC) than in DLPE (or PLPE), whereas there is no significant difference in the diene production (per linoleic chain) for these lipid dispersions. Since phospholipids in chloroform are suggested to exist in the monomeric state, a higher production efficiency of fluorophores in DLPE (or PLPE) can be explained by supposing a high effective local concentrations of reactive groups. This explanation is consistent with the observation that the production efficiency of fluorophores from DOPE/DLPC or DOPE/PLPC is higher in hexane than in chloroform; in the former solvent, phospholipids form reverse micelles.

It should be pointed out, however, that the production efficiency of fluorophores can be affected by many other factors. In order to explain a large difference in the production efficiency for DOPE/DLPC and DOPE/PLPC (or DLPE vs. PLPE), one needs to take account of differences in the number of linoleic chain per lipid. As the concentration of linoleic chain in DOPE/DLPC (or DLPE) is twice as high as that in DOPE/PLPC (or PLPC), one can expect at least a 2-fold production of fluorophores in the former system. Another factor that should be taken into account is the formation of very large aggregates of DLPE and PLPE in hexane, because their deposition to the wall of the test tube causes a substantial decrease in the lipid concentration in the bulk phase.

4.3. Characterization of fluorophores produced by lipid peroxidation

Although fluorescent products of DOPE/PLPC were separated into two major bands by TLC, these two major fluorescent components were suggested to be produced by the same reaction pathway; i.e., one of them is an intermediate product decomposing to the other component. The latter component exhibited an emission spectrum with a fine structure in the wavelength region between 400 nm and 500 nm (Fig. 2a). Such an emission spectrum is not seen in the literatures dealing with lipid peroxidation. So far, three possible structures have been proposed to describe fluorophores derived by peroxidation in the presence of amino compounds: the conjugated Schiff base [2], 1,4-dihydropyridine-3,5-dicarbaldehydes [3] and 8-(*N*-substituted-4,5-dihydro-4-oxo-5-hexyl-5-hydroxy-2-pyrrolyl)-octanoic acid methyl esters [4]. In these studies, water-soluble amino compounds were reacted with malonaldehyde (the former two compounds) or keto-oleic acid (the third one). It is not clear how the fluorophores produced by oxidation of amino phospholipids in organic solvents are related to the proposed structures.

When the hydrophobic environment within biomembranes is taken into consideration, one can expect that the reaction system used in the present study mimics some biological membrane systems. For instance, a reverse micellar structure has been suggested to be an intermediate structure within a biological membrane during fusion [10]. The production rate of fluorophores may be high in such a membrane region, because a recent study on peroxidation of unsaturated PC/PE mixtures shows that phospholipids in inverted hexagonal phase are more susceptible to peroxidation than those in lamellar phase [27].

Acknowledgements

This study was supported by a Special Researcher's Basic Science Program of Science and Technology Agency of Japan.

References

[1] Tappel, A.L. (1973) Fed. Proc. 32, 1870–1874.
[2] Chio, K.S. and Tappel, A.L. (1969) Biochemistry 8, 2821–2827.
[3] Kikugawa, K. and Ido, Y. (1984) Lipids 19, 600–608.
[4] Fukuzawa, K., Kishikawa, K., Tokumura, A., Tsukatani, H. and Shibuya, M. (1985) Lipids 20, 854–861.
[5] Shimasaki, H., Ueta, N., Mowri, H. and Inoue, K. (1984) Biochim. Biophys. Acta 792, 123–129.
[6] Koster, J.F. and Slee, R.G. (1980) Biochim. Biophys. Acta 620, 489–499.
[7] Jain, S.K. and Hochstein, P. (1980) Biochem. Biophys. Res. Commun. 92, 247–254.
[8] Esterbauer, H., Koller, E., Slee, R.G. and Koster, J.F. (1986) Biochem. J. 239, 405–409.
[9] Itoh, F., Horie, T. and Awazu, S. (1988) Arch. Biochem. Biophys. 264, 184–191.
[10] Siegel, D.P. (1987) In Cell Fusion (Sowers, A.E., ed.), pp. 181–207, Plenum Press, New York.
[11] Yamamoto, Y., Niki, E., Kamiya, Y. and Shimasaki, H. (1984) Biochim. Biophys. Acta 795, 332–340.
[12] Kates, M. (1986) Techniques of Lipidology, pp. 232–241, Elsevier Science, Amsterdam
[13] Kouyama, T., Kinosita, K. and Ikegami, A. (1989) Eur. J. Biochem. 182, 517–521.
[14] Kinosita, K., Jr. and Ikegami, A. (1984) In Subcellular Biochemistry (Hilderson, H.J., ed.), pp. 55–88, Plenum Press, New York.
[15] Fujisawa, T., Ueki, T., Inoko, Y. and Kataoka, M. (1987) J. Appl. Cryst. 20, 349–355.
[16] Guinier, A. and Fournet, G. (1955) Small-Angle Scattering of X-rays, pp. 24–28, John Wiley, New York.
[17] Gutteridge, J.M.C., Kerry, P.J. and Armstrong, D. (1982) Biochim. Biophys. Acta 711, 460–465.
[18] Gutteridge, J.M.C., Lunec, J. and Heys, A.D. (1978) Anal. Lett. A11, 537–544.
[19] Wittouck, N., Negri, R.M., Ameloot, M. and De Schryver, F.C. (1994) J. Am. Chem. Soc. 116, 10601–10611.
[20] Walde, P., Giuliani, A.M., Boicelli, C.A. and Luisi, P.L. (1990) Chem. Phys. Lipids 53, 265–288.
[21] Haque, R., Tinsley, I.J. and Schmedding, D. (1972) J. Biol. Chem. 247, 157–161.

[22] Barclay, L.R.C., MacNeil, J.M., VanKessel, J., Forrest, B.J., Porter, N.A., Lehman, L.S., Smith, K.J. and Ellington, J.C., Jr. (1984) J. Am. Chem. Soc. 106, 6740–6747.
[23] Whal, Ph. (1975) New Tech. Biophys. Cell Biol. 2, 233–241.
[24] Takagi, K., Suddaby, B.R., Vadas, S.L., Backer, C.A. and Whitten, D.G. (1986) J. Am. Chem. Soc. 108, 7865–7867.
[25] Barclay, L.R.C., Balcom, B.J. and Forrest, B.J. (1986) J. Am. Chem. Soc. 108, 761–766.
[26] Adams, G.E. and Wardman, P. (1977) In Free Radicals in Biology (Pryor, W.A., ed.), pp. 53–74, Academic Press, New York.
[27] Wang, J.Y., Miyazawa, T., Fujimoto, K., Wang, Z.Y. and Nozawa, T. (1992) FEBS Lett. 310, 106–110.